

# Absorption effects in the blazar’s $\gamma$ -ray spectra due to luminous stars crossing the jet

W. Bednarek & J. Sitarek

*University of Łódź, Department of Astrophysics, Faculty of Physics and Applied Informatics, ul. Pomorska 149/153, 90-236 Łódź, Poland, wladzimirz.bednarek@uni.lodz.pl; julian.sitarek@uni.lodz.pl*

Accepted . Received ; in original form

## ABSTRACT

$\gamma$ -ray emission in active galaxies is likely produced within the inner jet, or in the close vicinity of the supermassive black hole (SMBH) at sub-parsec distances.  $\gamma$  rays have to pass through the surrounding massive stellar cluster which luminous stars can accidentally appear close to the observer’s line of sight. In such a case, soft radiation of massive stars can create enough target for transient absorption of the  $\gamma$  rays in multi-GeV to TeV energy range. We consider the effect of such stellar encounters on the  $\gamma$ -ray spectrum produced within the massive stellar cluster surrounding a central SMBH. We predict characteristic, time-dependent effects on the  $\gamma$ -ray spectra due to the encounter with the single luminous star and also stellar binary system. We conclude that during the encounter, the  $\gamma$ -ray spectrum of an active galaxy should steepen at tens of GeV and harden in the range of hundreds of GeV. As an example, we consider such effects on the spectra observed from a typical blazar, 1ES 1959+650 (in an active state) and also in the case of a radio galaxy M87 (in a low state). It is shown that observation of such transient characteristic features in the  $\gamma$ -ray spectra, observed from blazars and radio galaxies, lays within the sensitivity of the future Cherenkov Telescope Array.

**Key words:** galaxies: active — galaxies: individual (1ES 1959+650, M87) — radiation mechanisms: non-thermal — gamma-rays: galaxies

## 1 INTRODUCTION

It is supposed that high-energy  $\gamma$  rays from active galaxies are produced within the inner jet or in the magnetosphere of the supermassive black hole (SMBH) due to their extremely short variability time scale. In fact, in the case of some blazars, the TeV  $\gamma$ -ray emission can change significantly on a time scale as short as minutes (e.g. Mrk 501, see Albert et al. 2007; PKS 2155-304, see Aharonian et al. 2007 or IC 310, see Aleksic et al. 2014), suggesting that the emission site has to be close to the SMBH, even if a mild relativistic boosting is taken into account. Also theoretical models for the high-energy  $\gamma$ -ray emission usually locate relativistically moving emission region at sub-parsec distances from the SMBH in order to correctly describe the spectral features (e.g. Bednarek & Protheroe 1997a, Tavecchio et al. 1998). Collimated  $\gamma$ -ray emission (a  $\gamma$ -ray beam) has to propagate through the surrounding region of the SMBH in which many compact objects are expected. The angular extend of such a beam in the blazar type of active galaxies,  $\alpha$ , is believed to be determined by the Lorentz factor of the inner jet which for  $\gamma_b \sim 10$  is  $\alpha \sim 1/\gamma_b \sim 0.1$  rad. However, in the case

of TeV  $\gamma$ -ray radio galaxies, the beams have to be much broader, or the jet has to be composed of a faster, more compact, and slower, more extend, part, since the inclination angles of such galaxies, in respect to the observer’s line of sight, are typically much larger than  $\sim 0.1$  rad. In fact, the inner radio jets in these sources are inclined at large angles to the line of sight, e.g. in Cen A  $i \sim (50 - 80)^\circ$  (Tingay et al. 2001) and  $i \sim (12 - 45)^\circ$  (Müller et al. 2014), in NGC 1275  $i \sim (30 - 55)^\circ$  (Walker et al. 1994, Vermeulen et al. 1994) or  $i \sim (65 \pm 16)^\circ$  (Fujita & Nagai 2017), and in M87  $i \sim (10 - 19)^\circ$  (Biretta et al. 1999). Therefore, their TeV  $\gamma$ -ray beam has to be much wider.

We propose that the beam of energetic  $\gamma$  rays, produced in the central regions of active galactic nuclei (AGNs), encounters luminous stars from time to time. Those stars form a quasi-spherical halo around the central super-massive black hole (see Fig. 1). As already noted in Bednarek et al. (2016), the current star formation rate in the radio galaxy Cen A ( $\sim 2 M_\odot \text{ yr}^{-1}$ ) is responsible for the formation of  $(6 - 12) \times 10^7 M_\odot$  of young stars. This star formation rate is expected to provide  $\sim 3 \times 10^5$  stars with masses above  $20 M_\odot$  (Wykes et al. (2014). Significant part of these stars should

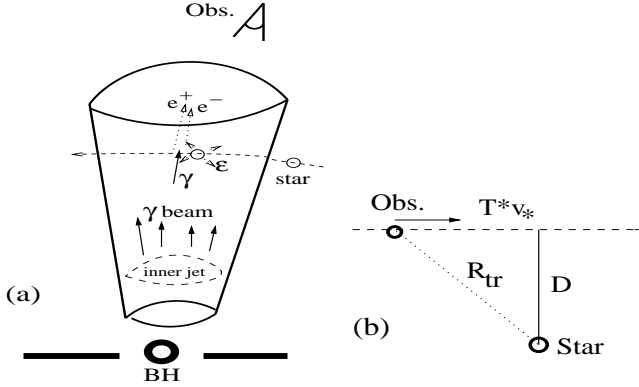


**Figure 1.** Schematic representation of the considered scenario for the production of specific absorption feature in the spectrum of GeV-TeV emitting active galaxies as seen in the active galaxy (figure a) and in the star reference frames (b). In (a): a  $\gamma$ -ray beam is produced in the inner part of the jet. It meets on its way the soft radiation of a luminous star which entered the jet.  $\gamma$  rays passing close by to the star are absorbed in soft radiation ( $\gamma + \epsilon \rightarrow e^+e^-$ ). As a result the absorption feature should appear in the broad band  $\gamma$ -ray spectrum produced in the inner jet. In (b): The observer’s (Obs) line of sight moves along the straight (dashed) line with the impact parameter  $D$ . At the time  $T$  (measured from the closest approach) the distance between the star and the observer is  $R_{\text{tr}}$ . The Observer location is defined by the product of the time  $T$  and the velocity of star  $v_*$ . The direction of the  $\gamma$ -ray beam is perpendicular to the plane of the drawing.

cross once in a while the jet pointing towards the observer. For the jet with simple conical geometry, the number of stars within the jet is estimated to be of the order of  $\sim 10^4 \theta_{20}^{-2}$ , where the jet half opening angle is normalized to  $\theta = 20 \theta_{20}$  degrees. Therefore, the interaction of the  $\gamma$ -ray beam, produced in the central part of the active galaxy with the radiation field of luminous stars around an active galaxy seems to be possible.

The number of transiting events clearly depend on the opening angle of the  $\gamma$ -ray beam from the vicinity of SMBH. The theoretical modelling of the  $\gamma$ -ray emission from the blazar type active galaxies usually postulate that it is collimated along the direction of a relativistic conical jet within the angle which is of the order of the inverse of the Lorentz factor of the jet (typically close to ten). However, it may not always be the case. The degree of collimation of the  $\gamma$ -ray emission is expected to be lower in the case of jets with other geometry (e.g. parabolic) or jets showing significant curvature, e.g. head-tail radio galaxies. Moreover, the off-axis  $\gamma$ -ray emission in radio galaxies is expected in the presence of two emission regions which exchange the radiation field (see Georganopoulos et al. 2005 and Banasiński & Bednarek 2018) and also in the inverse Compton (IC)  $e^\pm$ -pair cascade models in which the ordered magnetic field can re-distribute directions of secondary  $\gamma$ -rays outside the opening angle of the jet (e.g. Sitarek & Bednarek 2010, or Roustazadeh & Böttcher 2011). Off-axis TeV  $\gamma$ -ray emission is also expected to occur in the magnetosphere of the rotating super massive black hole (SMBH) (e.g. Rieger & Mannheim 2002, Neronov & Aharonian 2007, Rieger & Aharonian 2008, Levinson & Rieger 2011, Aleksić et al. 2014).

A class of scenarios for the high energy processes, in

which jets of active galaxies collide with compact objects, have been recently studied in detail. Different types of stellar objects can enter the jet from the massive stellar cluster surrounding SMBH (e.g. stars, clouds or even globular clusters, fragments of supernova remnants or pulsar wind nebulae). Collisions of the jet plasma with above-mentioned compact objects provide good conditions for acceleration of particles which can be responsible for the high-energy  $\gamma$ -ray emission (see e.g. Bednarek & Protheroe 1997b, Barkov et al. 2010, Bosch-Ramon et al. 2012, Araudo et al. 2013, Wykes et al. 2014, Bednarek & Banasiński 2015, Bosch-Ramon 2015, de la Cita et al. 2016, Banasiński et al. 2016, Vieyro et al. 2017, Torres-Alba et al. 2019).

We consider another aspect of the general encounter scenario between the  $\gamma$ -ray beam and luminous stars. It is assumed that the collimated beam of  $\gamma$  rays is already produced in the close vicinity of SMBH in one of the scenarios mentioned above. This  $\gamma$ -ray beam occasionally encounters compact luminous stars which pass close to the observer’s line of sight. As a result, a transient, broad feature is expected to appear in the continuum  $\gamma$ -ray spectrum due to the partial absorption of those  $\gamma$  rays in the thermal radiation of the star. Such transient feature is expected in the multi-GeV to sub-TeV  $\gamma$ -ray energies. It manifests itself as a hardening of the spectrum below  $\sim$ TeV energies and as a softening of  $\gamma$ -ray spectrum above  $\sim 10$  GeV. We propose that such effects can be transiently detected in the sub-TeV  $\gamma$ -ray spectra observed from active galaxies by Cherenkov telescopes (e.g. future Cherenkov Telescope Array, CTA).

Note that similar, but persistent absorption features in the multi-GeV  $\gamma$ -ray spectra of some optically violently variable type blazars, are also expected to appear in the case of very strong soft radiation field formed by the broad emission line regions around SMBHs (e.g. Poutanen & Stern 2010, Stern & Poutanen 2011, Abolmasov & Poutanen 2017). They might also effect the TeV  $\gamma$ -ray emission from BL Lac type active galaxies due to the absorption of  $\gamma$  rays in the infra-red radiation of molecular toruses (Protheroe & Biermann 1997, Donea & Protheroe 2003).

## 2 MASSIVE STARS THROUGH THE $\gamma$ BEAM

We assume that the  $\gamma$ -ray production region in the vicinity of the SMBH (either the inner jet or the black hole magnetosphere) is surrounded by a young massive cluster of stars (see Fig. 1). The  $\gamma$ -ray spectra from active galaxies are at first order well described by a simple power-law, or a log-parabola function through the GeV-TeV energy range. It is likely that some luminous stars pass close to the line of sight of a distant observer with a given impact parameter  $D$ , defined as the shortest distance between the line of sight and the centre of the star. During such passage, the dense radiation field of the star can partly absorb  $\gamma$  rays in a specific energy range. Since the stars move around SMBH with a significant velocity, the absorption effects should have transient nature.

We scale the typical parameters of the early type luminous stars with the surface temperature  $T_* \sim 3 \times 10^4 T_{4.5}$  K and the stellar radius  $R_* \sim 10^{12} R_{12}$  cm. Then, the optical depth is the largest for the  $\gamma$ -ray photons with energies,  $E_\gamma \sim 2m_e^2/\epsilon \sim 67/T_{4.5}$  GeV in the case of head on collisions.

It can be approximated by

$$\tau_{\gamma-\gamma}(r) \sim D n_{\text{ph}} \sigma_{\gamma-\gamma} \sim 110 R_{12} T_{4.5}^3 / r, \quad (1)$$

where  $\sigma_{\gamma-\gamma}$  is the cross section for  $e^\pm$  pair production in collision of two photons,  $n_{\text{ph}}$  is the density of stellar photons and  $r = D/R_\star$ . This rough estimation shows that  $\gamma$  rays moving at significant distances from the stellar surface can be absorbed.

The duration of the absorption effect on the  $\gamma$ -ray spectrum can be estimated for the known velocity of the luminous star on a circular orbit around the supermassive black hole. This velocity depends on the distance,  $R = 1R_1$  pc, of the star from the SMBH. It is given by,

$$v_\star \approx 9.4 \times 10^7 (M_8/R_1)^{1/2} \text{ cm s}^{-1}. \quad (2)$$

where  $M_{\text{SMBH}} = 10^8 M_8 M_\odot$  is the mass of the SMBH. Then, the characteristic minimum time scale of the stellar transit is of the order of  $\sim D/v_\star \sim 3r R_{12} (R_1/M_8)^{1/2}$  hours. Therefore, we expect that the  $\gamma$ -ray spectrum observed from active galaxies can be sporadically significantly modified in the multi-GeV to sub-TeV  $\gamma$ -ray energy range. We investigate the details of such effects on the  $\gamma$ -ray spectrum in the case of a transition of either a single or a binary system of two luminous stars close to the line of sight of a distant observer.

### 3 ABSORPTION EFFECTS DUE TO PASSAGE OF A SINGLE STAR

To analyse the effect of passage of a single star, we first compute the optical depth for  $\gamma$ -ray photons passing at different impact parameters to it. In the calculations we apply typical parameters of the O type and WR type stars. The optical depth is integrated along the direction towards the observer, which closest approach to the star is defined by the impact parameter  $D$ . We show that for typical parameters of luminous stars and impact parameters as large as  $D = (30 - 100)R_\star$ , the absorption of  $\gamma$  rays is still significant (see Fig. 2). For such large impact parameters, the simple power law  $\gamma$ -ray spectrum should still show a broad dip in the spectrum by a factor of a few at energies around  $\sim 50$ -200 GeV. The resulting softening and hardening of the source spectrum can be detected by Cherenkov telescopes sensitive in energy range of tens of GeV (e.g. such as MAGIC and future CTA).

The instantaneous distance of the  $\gamma$ -ray photons from the star can be calculated  $R_{\text{tr}} = \sqrt{D^2 + v_\star^2 T^2}$ , where  $T$  is the transit time measured from the closest approach of the star from the observer's line of sight (see Fig. 1b).

The absorption effect of the  $\gamma$ -ray spectrum in the radiation field of the star, during specific transit, can be evaluated by introducing the so-called "reduction factor" ( $RF$ ) which determines the ratio of integral  $\gamma$ -ray photon fluxes in specific range of energies  $E_{\text{min}} - E_{\text{max}}$ : with the effect of the absorption to the non-absorbed (intrinsic) one. The  $RF$  factor is defined as,

$$RF_{E_{\text{min}}} = \frac{\int_{E_{\text{min}}}^{E_{\text{max}}} (dN_\gamma/dE_\gamma) e^{-\tau} dE_\gamma}{\int_{E_{\text{min}}}^{E_{\text{max}}} (dN_\gamma/dE_\gamma) dE_\gamma}. \quad (3)$$

For the first calculations, we assume a differential  $\gamma$ -ray spectrum (produced either in the inner jet or in the vicinity of

the SMBH) of a power-law type with an index of  $-2$ , i.e.  $dN_\gamma/dE_\gamma \propto E_\gamma^{-2}$ , and the maximum energy at which the absorption effect of  $\gamma$  rays is still important.  $\tau$  is the optical depth for  $\gamma$  rays in the radiation field of the star as shown in Fig. 2. As an example,  $\log RF$  is calculated for the specific parameters of the luminous star (see legend in Fig. 3) and fixed impact parameters but for different velocities of the luminous stars  $v_\star$  and as a function of the transit time  $T$ , for two threshold energies  $E_{\text{min}} = 30$  GeV (Fig. 3a) and 300 GeV (Fig. 3b). The dependence of  $RF$  on  $E_{\text{min}}$ , for fixed stellar velocity and impact parameter, are shown in Fig. 3c. The typical transits, resulting in a significant absorption of  $\gamma$  rays, last for a few to several days for the considered parameters. In the case of a transit of a single star, the effect of  $\gamma$ -ray absorption in the stellar radiation is symmetrical.

We also show how the  $\gamma$ -ray spectra are modified at specific transit times by the absorption effects in the case of transiting single star (see Fig. 4). The broad absorption dip appears between a few tens of GeV and a few hundreds of GeV. As a result a part of the spectrum above  $\sim 10$  GeV should clearly steepen and a part of the spectrum in the sub-TeV energy range hardens. Such transient features, with characteristic time scales lasting from a few days up to a few tens of days, are predicted to appear in the observations of active galaxies using Cherenkov telescopes.

### 4 ABSORPTION EFFECTS DUE TO PASSAGE OF A BINARY SYSTEM

Half of the stars is expected to form binary systems. Therefore, we also consider the passage of luminous binary stellar system close to the observer's line of sight. In such a case, the effect of absorption of primary beam of  $\gamma$  rays can have much more complicated time dependence since the distances between the observer's line of sight and each of the stars is additionally modulated by the movement of stars within the binary system (for the schematic geometry see Fig. 5). For simplicity, we consider that the binary system contains two stars of equal mass. Then, the velocities of specific stars within the binary system are

$$v_\star = \left(\frac{GM_\star}{4a}\right)^{1/2} \approx 4.1 \times 10^6 \left(\frac{M_1}{a_{13}}\right)^{1/2} \text{ cm s}^{-1}, \quad (4)$$

where the radius of the binary system is  $a = 10^{13} a_{13}$  cm, and the masses of stars are  $M_\star = 10M_1 M_\odot$ . Note that for some parameters they can be of similar order as the transit velocities of the stars moving around the SMBH (see Eq. 2). In fact, the transit velocities of binary systems are limited by the condition of disruption of the binary system in the gravitational field of SMBH. We estimate the minimum distance of the binary system from the SMBH at which the tidal forces on stellar companions are balanced by gravitational force of companion stars on,

$$L \approx (16M_8/M_1)^{1/3} a \approx 1.8 \times 10^{-3} a_{13} (M_8/M_1)^{1/3} \text{ pc}. \quad (5)$$

We assume that most of the stellar binary systems in the central stellar cluster stay at distances from the SMBH that are larger than the above estimate.

The absorption effects of  $\gamma$  rays in the stellar radiation field strongly depend on the closest distance between the observer's line of sight and the centre of mass of luminous

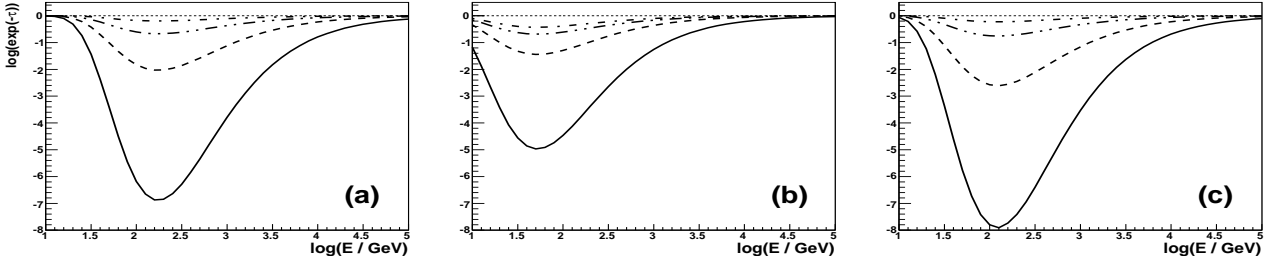


**Figure 2.** Optical depths for  $\gamma$  rays in the radiation field of stars with the parameters  $R_\star = 10^{12}$  cm and  $T_\star = 3 \times 10^4$  K (a) and  $R_\star = 2 \times 10^{11}$  cm and  $T_\star = 10^5$  K (b). In figure (a)  $\gamma$ -rays propagate along the straight line with the impact parameters are  $D = 3R_\star$  (solid curve),  $10R_\star$  (dashed),  $30R_\star$  (dot-dot-dashed),  $100R_\star$  (dot-dashed). In figure (b)  $D = 30R_\star$  (solid),  $100R_\star$  (dashed),  $200R_\star$  (dot-dot-dashed),  $300R_\star$  (dot-dashed). In figure (c), parameters of the star are those for WR 20a star ( $R_{\text{WR20a}} = 1.35 \times 10^{12}$  cm,  $T_{\text{WR20a}} = 4.3 \times 10^4$  K) and  $D = 10R_\star$  (solid),  $30R_\star$  (dashed),  $100R_\star$  (dot-dot-dashed),  $200R_\star$  (dot-dashed).

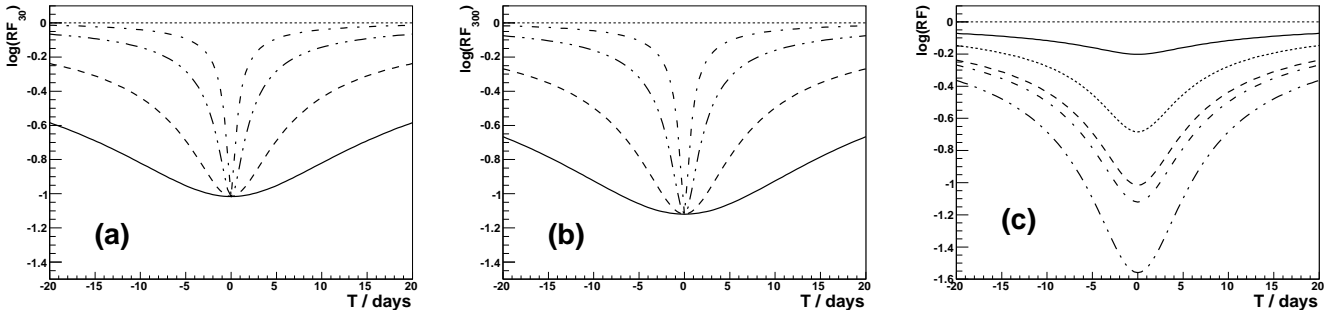


**Figure 3.** Log of the reduction factor (RF) of the  $\gamma$ -ray flux above 30 GeV (a) and 300 GeV (b) in the case of a star with the radius  $R_\star = 10^{12}$  cm and the surface temperature  $T_\star = 3 \times 10^4$  K. The star crosses the  $\gamma$ -ray beam with the impact parameter  $D = 10^{13}$  cm and with the velocity  $v_\star = 10^7$  cm s $^{-1}$  (solid curve),  $3 \times 10^7$  cm s $^{-1}$  (dashed),  $10^8$  cm s $^{-1}$  (dot-dot-dashed), and  $3 \times 10^8$  cm s $^{-1}$  (dot-dashed). The reduction factors for the star with the same parameters as in (a) and velocity  $v_\star = 3 \times 10^7$  cm s $^{-1}$  but for the  $\gamma$ -ray flux above 10 GeV (solid), 30 GeV (dashed), 100 GeV (dot-dashed), 300 GeV (dot-dot-dashed), and 1 TeV (dotted) are shown in (c).

stars, i.e. the impact parameter  $D_{\text{bin}}$ . Therefore, we calculate the distance between the line of sight and the centres of stars,  $D$ , for some specific parameters of the stars and transition event. The results are shown as a function of the transition time for the example values of the impact parameter,  $D_{\text{bin}}$ , different velocities of transiting binary system,  $v_\star$ , and radii of the binary system,  $a$ , for fixed phase of the binary  $\phi = 0^\circ$  (see Fig. 6). On the other hand, the dependence of this distances on the phase of the binary,  $\phi$ , is shown in Fig. 7. Note the fast dependence of the impact parameters of individual stars on the transit time  $T$ . During several days, those distances can change by an order of magnitude. They show double-peak structure due to the transiting two stars within the binary systems. Similar interesting effects are expected to appear in the  $\gamma$ -ray spectra influenced by the absorption of the  $\gamma$ -ray beam in the radiation field of such a binary system.

The cumulative effect of absorption of  $\gamma$  rays (expressed by the reduction factor  $RF$ ) in the radiation of stars in the example transiting binary system are shown in Fig. 8 for the case of two threshold energies  $E_{\text{min}} = 30$  GeV (upper figures) and 300 GeV (lower figures). The simplest binary system case, namely two identical stars with the orbital plane perpendicular to the direction of the  $\gamma$ -ray beam, is considered. We show the absorption effects for the case of four impact parameters,  $D_{\text{bin}} = 10^{13}$  cm,  $5 \times 10^{12}$  cm,  $-5 \times 10^{12}$

cm, and  $-10^{13}$  cm, and the initial phase  $\phi = 0^\circ$  (see Fig. 5). The negative distances of the impact parameters denote opposite rotation direction of the stars than marked in Fig. 5.

The significant reduction of the  $\gamma$ -ray emission is predicted to occur on a time scale of a few tens of days. However, a strong reduction of the  $\gamma$ -ray flux, in the form of characteristic two strong absorption dips, is also expected on a time scale of a few days when the observer's line of sight comes close to the stars within the binary system.

We also calculate the effect of absorption on the spectrum of the  $\gamma$ -ray beam (see Fig. 9), for the case of the example binary system considered above. Interesting dependence of the spectrum on the transiting time can be observed. The basic feature, softening of the multi-GeV part of the spectrum and hardening of the sub-TeV part of the spectrum, can appear regularly during the transition event close to the minimum approach of the observer's line of sight. For the considered transition event, the effects of absorption are so strong that the  $\gamma$ -ray flux of the  $\gamma$ -ray beam can be drastically reduced. It can easily fall below the sensitivity limits of the  $\gamma$ -ray telescopes in this energy range. Note that considered here effects should strongly depend on the geometry of the binary system in respect to the observer's line of sight which greatly enhances the possibility of different absorption effects. Here we consider only the simplest possible geometry of the binary system, i.e. it is composed of two equal-mass

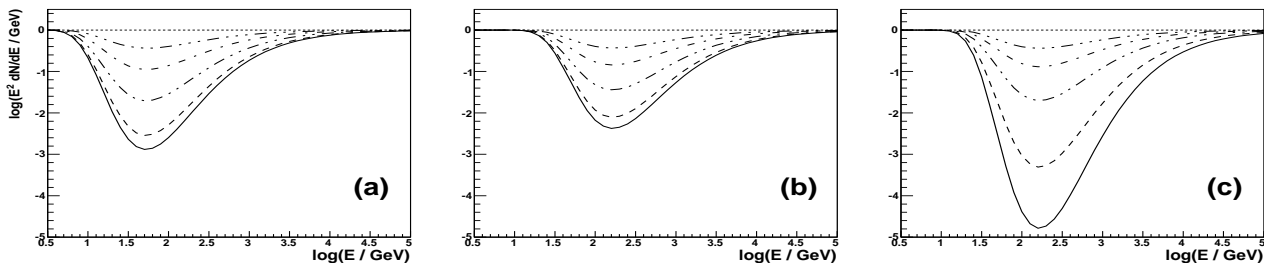


**Figure 4.** Gamma-ray spectra at different transit times  $T = -20$  days (dot-dot-dot-dashed curve),  $-10$  days (dot-dashed),  $-5$  days (dot-dot-dashed),  $-2$  days (dashed),  $0$  days (solid), in the case of a transit due to the single star with the parameters: the stellar radius  $R_* = 2 \times 10^{11}$  cm, the surface temperature  $T_* = 10^5$  K, and the observer transiting with the impact parameter  $D = 10^{13}$  cm and the velocity  $v_* = 3 \times 10^7$  cm s $^{-1}$  (figure a);  $R_* = 10^{12}$  cm,  $T_* = 3 \times 10^4$  K,  $D = 10^{13}$  cm and  $v_* = 3 \times 10^7$  cm s $^{-1}$  (b), and for the parameters as in (b) but for  $D = 5 \times 10^{12}$  cm (c).

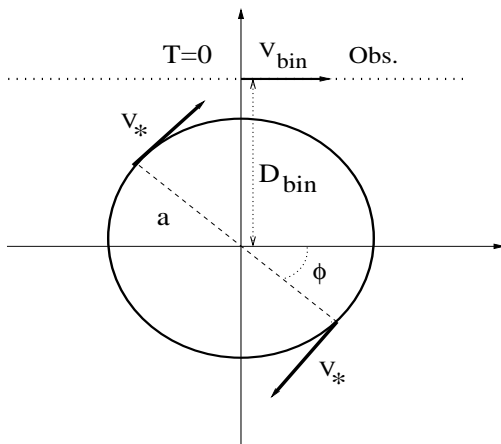


**Figure 5.** Schematic representation of the passage of a binary system through the  $\gamma$ -ray beam with the impact parameter  $D$  in the reference frame of the binary system centre of mass. The observer (Obs.) moves with a velocity  $v_{\text{bin}}$  along a straight line (dotted). The binary system contains two equal mass stars which move with velocity  $v_*$  on a circular orbit with the radius  $a$ . The orbit of the binary system lays in the plane perpendicular to the direction of the observer. The phase of the stars is marked by  $\phi$ . The time is measured from the closest distance between the observer and the centre of the binary system.

stars and its plane lays in the plane of the sky. However, in general, the plane of the binary system can be inclined at an arbitrary angle to the plane of the sky. Moreover, the binary system can be formed from two luminous stars which significantly differ in their basic parameters (stellar mass and temperature, binary radius). Therefore, we expect even more complicated structures in the light curve of the transition of binary stars through the  $\gamma$ -ray beam formed close to the central engine of active galaxy.

## 5 EFFECTS ON SPECIFIC SOURCES

As an example, we consider the absorption effects on the  $\gamma$ -ray spectra due to the transiting binary system through the  $\gamma$ -ray beam in the case of two well known active galaxies from which GeV-TeV  $\gamma$ -ray emission have been reported by

the *Fermi*-LAT and Cherenkov telescopes. The first active galaxy is a BL Lac object: 1ES 1959+650. Recently it was detected in the high state by the *Fermi*-LAT in the multi-GeV energies and by MAGIC in sub-TeV energies (Acciari et al. 2020b). We include the effects of absorption of  $\gamma$ -ray spectra observed from 1ES 1959+650 in the case of transits of two binary systems with likely binary system and transit parameters (see left columns of Fig. 10). The modifications of the  $\gamma$ -ray spectrum by the transiting binary system at a specific time before minimum distance between the centre of the binary system and the observer's line of sight are shown for  $T = -20 - 0$  days. We also consider the effect of a transit of the binary system on the spectrum of the well known radio galaxy M87 detected in a low state (Acciari et al. 2020a). As in the case of 1ES 1959+650, the transits of two binary systems with such parameters are considered. Expected modifications of the GeV to TeV  $\gamma$ -ray spectrum are reported in the middle column of Fig. 10.

We confront these modified  $\gamma$ -ray spectra with the sensitivities of the  $\gamma$ -ray ground-based and space instruments. We used the publicly available instrument response functions (IRF) `prod3b-2`<sup>1</sup> of the CTA Bernlöhner et al. (2013). For the stronger source, 1ES1959+650 we use short term (30 min) sensitivity IRF, while for a weaker M87 we use the corresponding mid-term (5 hr) IRF. Moreover, for 1ES1959+650 we also take into account the absorption in the extragalactic background light following Domínguez et al. (2011) model, which affects the observed emission from the source in the multi-TeV range. Using a given flux model, the collection area of the instrument, and its migration matrix, we determine the expected excess rates in each estimated energy bin. With such computed expected number of observed  $\gamma$  rays, and the rate of background events obtained from CTA IRF we estimate the expected uncertainty of the reconstructed flux. We consider that the flux can be probed at a given energy if the expected uncertainty is below 50% of the flux (i.e. resulting with  $> 2\sigma$  point) and the expected number of  $\gamma$  rays in this energy bin is above 10. In the case of 1ES 1959+650 it is clear that even very short ( $\sim 30$  min) exposure can be used for very accurate probing of the source spectrum and reproducing the absorption feature with high details. In the case of the much weaker M87 emission, while

<sup>1</sup> <https://www.cta-observatory.org/science/cta-performance/>

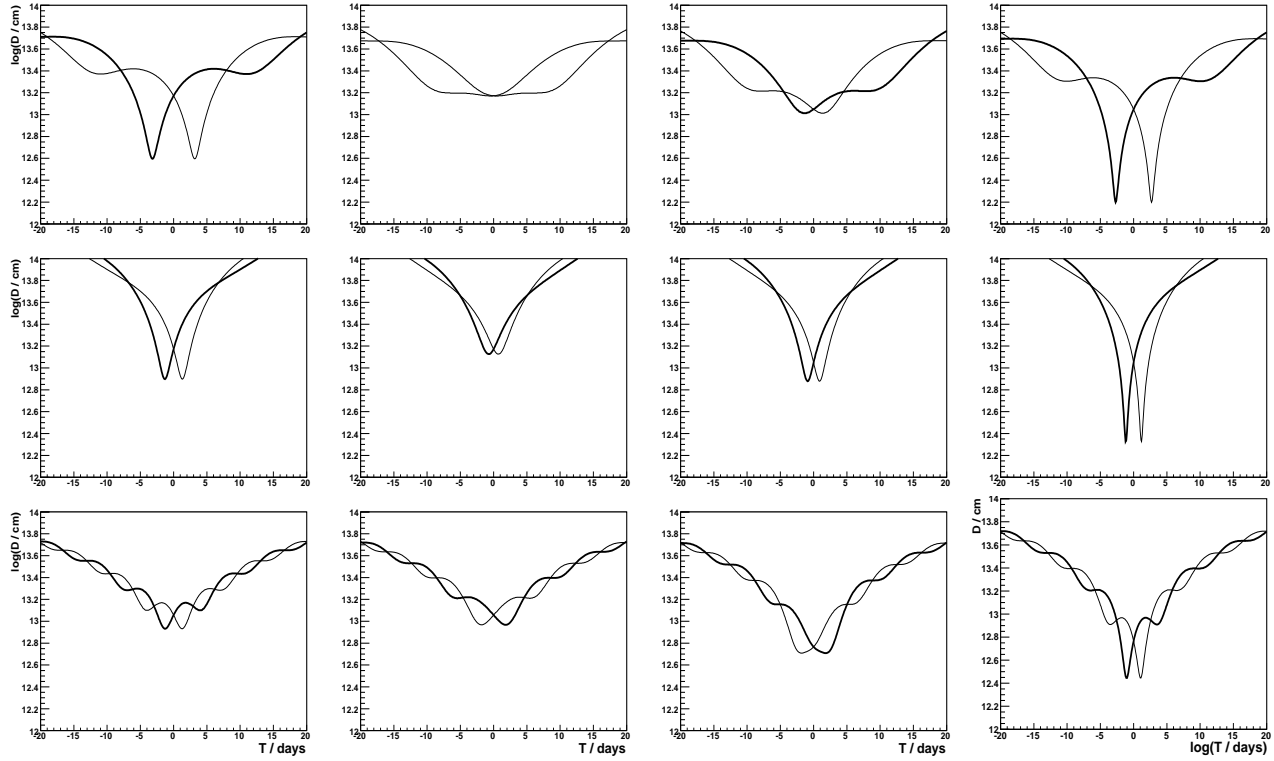


**Figure 6.** Distance,  $D$ , between the observer's line of sight and the first star (see thick curves) and the second star (thin curve) forming the binary system. The binary passes with the impact parameter  $D_{\text{bin}} = -1.1 \times 10^{13}$  cm (left column),  $1.1 \times 10^{13}$  cm (left-central column),  $5 \times 10^{12}$  cm (right-central), and  $-5 \times 10^{12}$  cm (right). The parameters of the binary system are: radius of stars  $R_{\star} = 10^{12}$  cm, the surface temperature  $T_{\star} = 3 \times 10^4$  K, semimajor axis  $a = 10^{13}$  cm, and the velocity of the stars  $v_{\star} = 3 \times 10^7$  cm s $^{-1}$ . The velocity of the binary system is  $v_{\text{bin}} = 3 \times 10^7$  cm s $^{-1}$  (upper panel) and  $v_{\text{bin}} = 10^8$  cm s $^{-1}$  (middle panel). The case with the parameters of the binary system is  $\phi = 0^{\circ}$ .

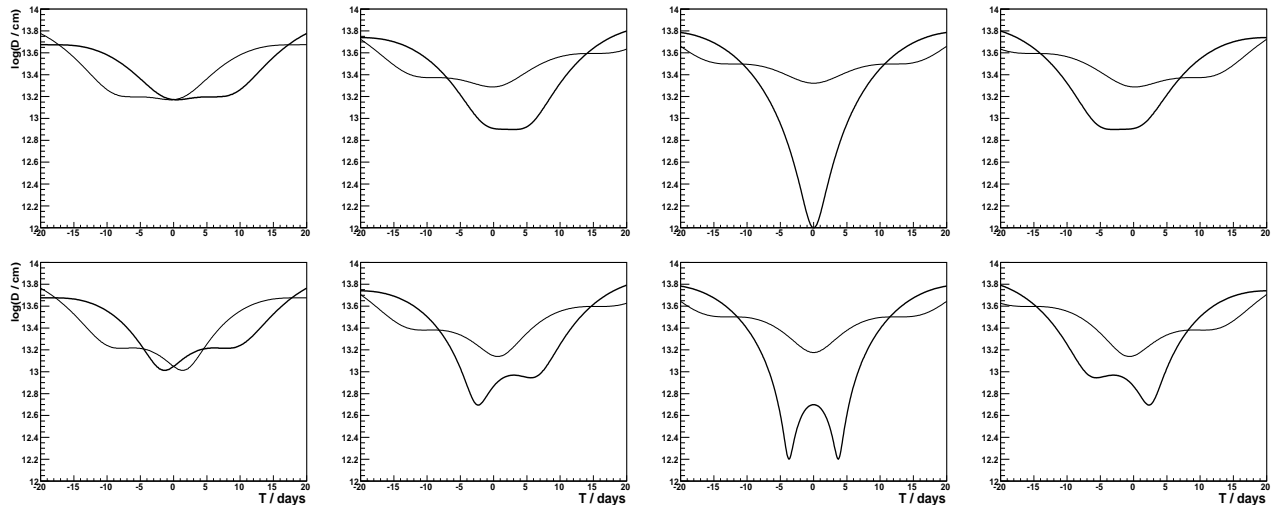


**Figure 7.** Dependence of the distances,  $D$ , between the stars and the direction to the observer's line of sight on the phase of the binary system  $\phi$  is shown for the parameters as in Fig. 6 in the upper panel and the impact parameter  $D_{\text{bin}} = 1.1 \times 10^{13}$  cm (upper panel) and  $D_{\text{bin}} = 5 \times 10^{12}$  cm (bottom panel):  $\phi = 0^{\circ}$  (left column),  $45^{\circ}$  (left-centre),  $90^{\circ}$  (right-centre), and  $135^{\circ}$  (right). The parameters of the binary system are  $v_{\text{bin}} = 3 \times 10^7$  cm s $^{-1}$ ,  $v_{\star} = 3 \times 10^7$  cm s $^{-1}$ ,  $a = 10^{13}$  cm. The binary system is composed from two stars with parameters  $R_{\star} = 10^{12}$  cm and  $T_{\star} = 3 \times 10^4$  K.

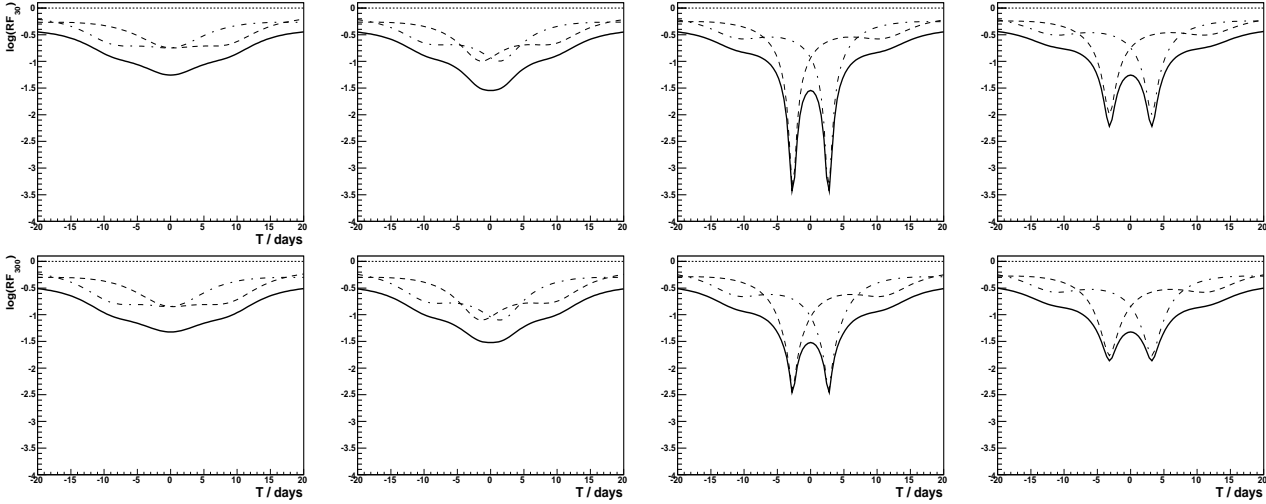


**Figure 8.** Effect of the transition of the stellar binary system on the  $\gamma$ -ray flux above 30 GeV (see  $\log RF_{30}$  on the upper figures) and above 300 GeV (see  $\log RF_{300}$  on the bottom figures). The parameters of the binary system are the following: stellar radius  $R_\star = 10^{12}$  cm, surface temperature  $T_\star = 3 \times 10^4$  K, semimajor axis  $a = 10^{13}$  cm, stellar velocity on the binary orbit  $v_\star = 3 \times 10^7$  cm s $^{-1}$ . Specific figures show the results for different impact parameters  $D_{\text{bin}} = 1.1 \times 10^{13}$  cm (on the left figures),  $5 \times 10^{12}$  cm (left-centre),  $-5 \times 10^{12}$  cm (right-centre), and  $-1.1 \times 10^{13}$  cm (right). The  $\gamma$ -ray beam has the differential power law spectrum with the spectral index -2.

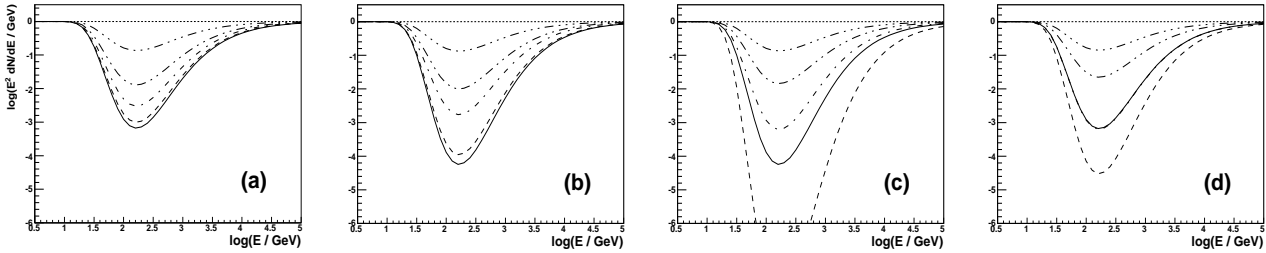


**Figure 9.** Absorption effect on a simple spectrum of the  $\gamma$ -ray emission (differential power law spectrum multiplied by energy squared) at different transit times,  $T = -20$  days (dot-dot-dot-dashed),  $-10$  days (dot-dot-dashed),  $-5$  days (dot-dashed),  $-2$  days (dashed),  $0$  days (solid) for the parameters: (a) the binary system of two stars (with stellar radius  $R_\star = 10^{12}$  cm, surface temperature  $T_\star = 3 \times 10^4$  K, semimajor axis  $a = 10^{13}$  cm, stellar velocity on the binary orbit  $v_\star = 3 \times 10^7$  cm s $^{-1}$ ) passes the  $\gamma$ -ray beam with the velocity of the binary  $v_{\text{bin}} = 3 \times 10^7$  cm s $^{-1}$ , and the impact parameter  $D_{\text{bin}} = 1.1 \times 10^{13}$  cm (see a),  $D_{\text{bin}} = 5 \times 10^{12}$  cm (b),  $D_{\text{bin}} = -5 \times 10^{12}$  cm (c), and  $D_{\text{bin}} = -1.1 \times 10^{13}$  cm (d). See Fig. 5, for the location of the binary in respect to the plane of the sky.

the intrinsic spectrum can be reconstructed without the stellar absorption (the emission is at the border of differential sensitivity for 5 hr exposures), the absorption in stellar radiation would render the emission undetectable close to the transit time. For M87 we perform additional calculations to evaluate at which statistical level the occurrence of the absorption can be probed for a given observation time. For each  $i$ -th energy bin that is measurable in the non-absorbed spectrum ( $F_{0,i} \pm \Delta F_{0,i}$ ) we compute their flux and uncertainty for a given absorption conditions ( $F_{\tau,i} \pm \Delta F_{\tau,i}$ ). We then compute:

$$\chi^2 = \sum_{i=1}^N \left( 1 + \frac{(F_{\tau,i} - F_{0,i})^2}{\Delta F_{\tau,i}^2 + \Delta F_{0,i}^2} \right) \quad (6)$$

Note that '1' is added in summation to simulate the effect of the fluctuations of the measured fluxes. We then compute the corresponding probability as the  $\chi^2$  distribution with  $N$  degrees of freedom integrated above  $\chi^2$  (the values for M87 are given in the right columns of Fig. 10). Such prob-

ability can be interpreted as the chance probability related to detection of an absorption feature by future CTA observations. Curiously, it is easier to detect strong absorption as a sudden lack of detectable flux by CTA, however in this case the ability to extract the physical parameters of the absorbing star/system from the sub-TeV data would be clearly reduced.

We investigate if the softening of the  $\gamma$ -ray spectrum at energies of tens of GeV can be observed by *Fermi*-LAT Atwood et al. (2009). We used the publicly available *Pass8* collection area<sup>2</sup> to judge the achieved performance for a 10-day exposure of the *Fermi*-LAT instrument. We find that even for a high flux level comparable to the 1ES 1959+650 high state, even without the absorption of the  $\gamma$  rays in the stellar radiation field, the sensitivity of the instrument does not allow to significantly probe the emission of the source

<sup>2</sup> [https://www.slac.stanford.edu/exp/glast/groups/canda/lat\\_Performance.htm](https://www.slac.stanford.edu/exp/glast/groups/canda/lat_Performance.htm)

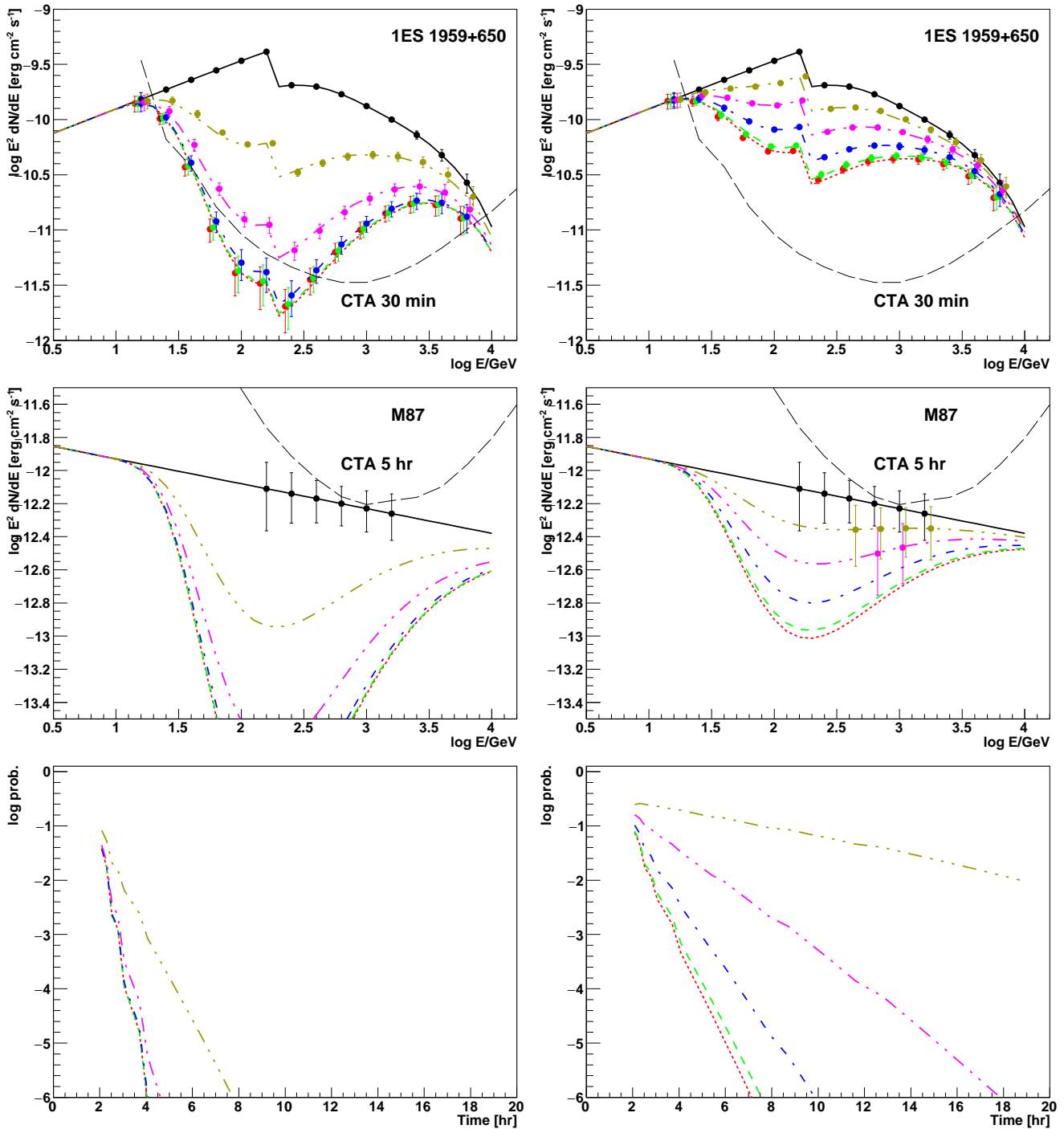


**Figure 10.** Effect of absorption on the  $\gamma$ -ray spectrum observed from two active galaxies: BL Lac 1ES 1959+650 (in the high emission state, see Acciari et al. 2020b, including the absorption in extragalactic background light using Domínguez et al. 2011 model) and the radio galaxy M87 (in the low state, see Acciari et al. 2020a). The absorption effect due to the passing binary system of stars with the parameters  $R_\star = 10^{12}$  cm,  $T_\star = 3 \times 10^4$  K,  $a = 10^{13}$  cm,  $D_{\text{bin}} = 2 \times 10^{13}$  cm,  $v_\star = 3 \times 10^7$  cm s $^{-1}$ , and  $v_{\text{bin}} = 3 \times 10^7$  cm s $^{-1}$  through the  $\gamma$ -ray beam is shown for 1ES 1959+650 (top left) and M87 (center left) for the parameters,  $R_\star = 10^{12}$  cm,  $T_\star = 3 \times 10^4$  K,  $a = 10^{13}$  cm,  $D_{\text{bin}} = 5 \times 10^{13}$  cm,  $v_\star = 3 \times 10^7$  cm s $^{-1}$ . The transition events with  $v_{\text{bin}} = 10^8$  cm s $^{-1}$  are shown for 1ES 1959+650 (top right) and M87 (center right). The spectra with absorption features correspond to different time measured in respect to the closest distance between the centre of the binary system and the direction to the observer:  $T = 0$  days (dotted red curve), -2 days (dashed green), -5 days (dot-dashed blue), -10 days (dot-dot-dashed magenta), and -20 days (dot-dot-dot-dashed olive). The spectra are confronted with the 0.5 hr (for 1ES 1959+650) or 5 hr (for M87) sensitivity of CTA (see text). Points and uncertainties show the expected range and accuracy of the reconstructed spectrum by CTA for the given observation time with CTA (the points are slightly shifted between each curve for clarity). The bottom row shows the chance probability corresponding to detection of absorption feature in M87 for  $v_{\text{bin}} = 3 \times 10^7$  cm s $^{-1}$  (bottom left) and  $v_{\text{bin}} = 10^8$  cm s $^{-1}$  (bottom right) as a function of observation time.



above  $\sim 10$  GeV, where most of the effect is expected. Nevertheless, simultaneous observations in GeV range by satellite experiment to the observations in the sub-TeV range by Cherenkov telescopes would be still strongly desirable, since they can be used to constrain intrinsic source variability.

It is concluded that the CTA should easily detect the broad absorption feature between  $\sim 30$  GeV and  $\sim 1$  TeV (i.e. steepening of the part of the spectrum at lower energies and its hardening at larger energies) even during short observations. For bright sources, such effects might be even detected already with the current generation of Cherenkov telescopes. While, the detection of such effects in the low state emission of radio galaxies is also in reach of CTA, it would require to monitor source with deep (a few hours per night) exposures.

## 6 DISCUSSION AND CONCLUSION

We considered the effects of transition of luminous stars (single or within the binary system) through the  $\gamma$ -ray beam produced in the direct surrounding of the SMBH, i.e. either in the SMBH magnetosphere or in the inner part of the jet. It is assumed that from time to time stars pass close to the line of sight of a distant observer. If the transition is closer than hundreds of stellar radii of a luminous star, the  $\gamma$  rays from primary  $\gamma$ -ray beam are partially absorbed. As a result, a broad dip at multi-GeV to sub-TeV range should appear in the continuous  $\gamma$ -ray spectral energy distribution produced around SMBH. This dip should be observed by the Cherenkov telescopes as a significant steepening of the spectrum above  $\sim 10$  GeV and as a hardening of the spectrum below  $\sim$ TeV energies. Such a combined feature is characteristic, and hence can be easily disentangled from a possible intrinsic variability of the  $\gamma$ -ray beam. The time scale of such a transition event should depend on the distance of the transiting star from the SMBH. It is predicted to take typically a few to a few tens of days. Therefore, it is expected that such events might be detected with the help of the current and future Cherenkov telescopes.

As an example, we apply our calculations to two well known active galaxies. In the case of the BL Lac type active galaxy 1ES 1959+650, we show that in its high state the effect of  $\gamma$ -ray absorption can be easily observed by the CTA telescopes (under construction) in the sub-TeV energy range during a few days (see Fig. 10) even with very short nightly exposures. We also investigate the case of radio galaxy M87 in the low emission state. With enough exposure, CTA would be able to observe a clear hardening of the  $\gamma$ -ray spectrum at sub-TeV energies. In fact, for bright sources detection of such an absorption feature might be even possible with the present generation of Cherenkov telescopes (H.E.S.S., MAGIC and VERITAS) which sensitivity is nearly an order of magnitude lower than CTA. Unfortunately, in neither of the two simulated cases *Fermi*-LAT is sensitive enough to detect such absorption feature.

Detection of such transiting events (or their lack) should provide interesting constraints on the parameters of the central stellar clusters in active galaxies and on the production site of the  $\gamma$ -ray emission in active galaxies. Note that the duration of transition depends on the velocity of transiting stars which depends on the distance from SMBH, provided

that its mass is known. On the other hand, the frequency of detected transiting events should allow us to constrain the distribution function of luminous stars in the central stellar cluster. The temperature of the star in turn affects strongly the depth of the dip in the spectral energy distribution and its position. In the case of transiting binary systems of two luminous stars, the time structure of transition should have curious features containing double peak structure with very fast change of the absorption efficiency (see Fig. 8). Observation of such double peaked absorption structures will allow us to constrain the surviving frequency of binary stellar systems in the direct vicinity of the SMBH. Therefore, the observations of transition events via sub-TeV absorption can be used to study the basic parameters of the stars in extreme conditions of neighbourhood of SMBH.

In principle, more than a single star (or a single binary system) can accidentally appear close to the observer's line of sight within the jet. Then, the effects considered in the previous section will become much more complicated. Even two absorption features, depending on the surface temperatures of the transiting stars, might appear in the gamma-rays spectrum observed from active galaxy. Also, predicted  $\gamma$ -ray light curves will become very complicated. However, we expect that such multiple encounters happen very rarely since the stars have to not only stay within the jet but also relatively close to the observer's line of sight.

As a result of absorption of  $\gamma$  rays in the stellar radiation, secondary leptons with sub-TeV energies will appear in the volume around luminous stars. We expect that those leptons will be effectively removed from the direction towards the observer. Their typical Larmor radii are  $R_L = 3 \times 10^8 \gamma_{55} / B_G$  cm, where  $\gamma_{\pm} = 3 \times 10^5 \gamma_{55}$  is the Lorentz factor of leptons, and  $B = 1 B_G$  G is the magnetic field strength at the location of the star. In our case the typical Lorentz factors of leptons are expected to be of the order of  $3 \times 10^5$  (note the location of the absorption dip). The mean free path of leptons on the synchrotron process in the magnetic field is  $\lambda_{\text{syn}} \approx 7.5 \times 10^{12} / (B_G^2 \gamma_{55})$  cm. Their mean free path for energy losses on the IC process in the Thomson regime is  $\lambda_{\text{IC}} \approx 3 \times 10^9 r_1^2 / (T_{4.5}^4 \gamma_{55})$  cm, where  $r_1 = r/10$  with  $r$  defined below Eq. 1. The magnetic field strengths in jets of AGNs at sub-parsec distances from the SMBHs are expected to be of the order of a Gauss. Similar order of the magnetic fields are also expected in the vicinity of massive stars. In fact, WR and O type stars have the surface magnetic fields as strong as  $\sim (1 - 3) \times 10^3$  G on the surface. When we apply such parameters in our calculations, then the Larmor radius of secondary leptons becomes shorter than their typical mean free paths for energy losses on the synchrotron and the IC processes. Therefore, the radiation from secondary leptons should be isotropised, i.e. mainly produced outside the direction towards the observer. Small excess of X-ray synchrotron emission should be expected in other directions with typical energies around,

$$\varepsilon \approx m_e c^2 (B/B_{\text{cr}}) \gamma^2 \approx 1.2 B_G \gamma_{55}^2 \text{ keV}, \quad (7)$$

where  $B_{\text{cr}} = 4.4 \times 10^{13}$  G is the critical magnetic field strength. On the other hand, energies of  $\gamma$  rays from the IC process of the secondary leptons should be comparable to those of  $\gamma$  rays absorbed in the primary  $\gamma$ -ray beam, i.e. in the GeV-TeV energy range. The small excess of secondary radiation, emitted in much broad solid angle, will be

rather difficult to distinguish from the primary beam of non-thermal emission from the central region of active galaxy.

In principle, considered above absorption features can also appear at about an order of magnitude larger energies (TeV  $\gamma$ -ray energy range) in the case of transiting red hyper- and super-giants. Their typical radii and surface temperatures are  $R_{RG} \sim 10^3 R_{\odot}$  and  $T_{RG} \sim 3000$  K. Then, the optical depth becomes of the order of unity already at the distance from the star  $D \sim 10 R_{RG}$  (see Eq. 1). In fact, large number of red giants is expected around SMHBs. For example, in the case of Cen A the number of red giants around SMBH is estimated on  $\sim 10^6$  (see Wykes et al. 2014 and the estimate in Banasiński et al. 2016). The  $\gamma$ -ray emission of blazars is detected at the angle a factor of a few larger than the intrinsic opening angle of the jet (e.g. Pushkarev et al. 2009). Therefore, red giants can transit outskirts of such a  $\gamma$ -ray beam, avoiding disruption by the jet pressure (as considered by e.g. Barkov et al. 2010), but affecting the broad  $\gamma$ -ray beam at the TeV energy range with their thermal radiation field.

## ACKNOWLEDGMENTS

We would like to thank the referee for useful comments. This work is supported by the grant through the Polish National Research Centre No. 2019/33/B/ST9/01904. This research has made use of the CTA instrument response functions provided by the CTA Consortium and Observatory, see <https://www.cta-observatory.org/science/cta-performance/> (version prod3b-v2) for more details.

## DATA AVAILABILITY

The simulated data underlying this article will be shared on reasonable request to the corresponding author.

## REFERENCES

- Abolmasov, P., Poutanen, J. 2017 MNRAS 464, 152  
 Acciari, V.A. et al. 2020a MNRAS 492, 5354  
 Acciari, V.A. et al. 2020b A&A 638, 14M  
 Aharonian, F. et al. 2007 ApJ 664, L71  
 Albert J. et al. 2007, ApJ 669, 862  
 Aleksić, J., Ansoldi, S., Antonelli, L.A. et al. 2014 Science, 346, 1080A  
 Araudo, A.T., Bosch-Ramon, V., Romero, G.E. 2013, MNRAS, 436, 3626  
 Atwood, W. B., Abdo, A. A., Ackermann, M., et al. 2009, ApJ, 697, 1071  
 Barkov, M.V., Aharonian, F.A., Bosch-Ramon, V. 2010, ApJ, 724, 1517  
 Banasiński, P., Bednarek, W. 2018, ApJ 864, 128  
 Banasiński, P., Bednarek, W., Sitarek, J. 2016 MNRAS 463 L26  
 Bednarek, W., Banasiński, P. 2015 ApJ 807, 168  
 Bednarek, W., Protheroe, R.J. 1997 MNRAS 292, 646  
 Bednarek, W., Protheroe, R.J. 1997 MNRAS 287, L9  
 Bernlöhr, K., Barnacka, A., Becherini, Y., et al. 2013, Astroparticle Physics, 43, 171. doi:10.1016/j.astropartphys.2012.10.002  
 Biretta, J.A., Parks, W.B.S., Acchetto, F.M. 1999 ApJ 520, 621  
 Bosch-Ramon, V. 2015 A&A 575, A109  
 Bosch-Ramon, V., Perucho, M., Barkov, M. V. 2012, A&A, 539,69  
 de la Cita, V.M., Bosch-Ramon, V., Paredes-Fortuny, X., Khangulyan, D., Perucho, M. 2016, A&A, 591, 15D  
 Domínguez, A., Primack, J. R., Rosario, D. J., et al. 2011, MNRAS, 410, 2556  
 Donea A-C., Protheroe, R.J. 2003 APh 18, 377  
 Funk, S., Hinton, J.A. 2013 APh 43, 333  
 Georganopoulos, M., Perlman, E.S., Kazanas, D. 2005 ApJ, 634, L33  
 Levinson, A., Rieger, F. 2011 ApJ 730, 123  
 Maier, G. et al. 2017, Proc. 35th ICRC (Busan, Korea), POS(ICRC2017), 846  
 Müller, C. et al. 2014, A&A 569, 115  
 Neronov, A., Aharonian, F.A. 2007 ApJ 671, 85  
 Poutanen J., Stern B., 2010 ApJ 717, L118  
 Protheroe, R.J., Biermann, P.L. 1997 APh 6, 293  
 Pushkarev, A.B., Kovalev, Y.Y., Lister, M.L., Savolainen, T. 2009 A& A 507, L33  
 Rieger, F.M., Aharonian, F.A. 2008 A&A 479, L5  
 Rieger, F.M., Mannheim, K. 2002, A&A, 396, 833  
 Roustazadeh, P., Böttcher, M. 2011 ApJ 728, 134  
 Sitarek, J., Bednarek, W. 2010, MNRAS, 401, 1983  
 Stern B. E., Poutanen J., 2011 MNRAS 417, L11  
 Tavecchio, F., Maraschi, L., Ghisellini, G. 1998 ApJ 509, 608  
 Tingay, S.J., Preston, R.A., Jauncey, D.L. 2001 AJ 122, 1697  
 Torres-Alba, N., Bosch-Ramon, V., 2019 A& A 623, 91  
 Vermeulen, R.C., Readhead, A.C.S., Backer, D.C. 1994 ApJ 430, 41  
 Vieyro, F.L., Torres-Albà, N., Bosch-Ramon, V. 2017 A&A 604, 57  
 Wykes, S., Hardcastle, M.J., Karakas, A.I., Vink, J.S. 2014, MNRAS, 442, 2867